PERGAMON

Atmospheric Environment 37 (2003) 4179–4194

ATMOSPHERIC ENVIRONMENT

www.elsevier.com/locate/atmosenv

Comparison of photochemical mechanisms for air quality modeling

Pedro Jimenez[a], Jose M. Baldasano[a], Donald Dabdub[b,*]

[a] *Environmental Modeling Laboratory, Universitat Politècnica de Catalunya, Avda. Diagonal, 647, Planta 10, Barcelona 08028, Spain*
[b] *Department of Mechanical and Aerospace Engineering, Henry Samueli School of Engineering, University of California at Irvine, Irvine, CA 92697-3975, USA*

Received 18 February 2003; accepted 7 July 2003

Abstract

Photochemical mechanisms are a critical module of air quality models. In the past 20 years, several mechanisms have been developed to study the chemistry of the troposphere. This work compares several state-of-the-science photochemical mechanisms (including LCC, CBM-IV, RADM2, EMEP, RACM, SAPRC99, and CACM which have never been compared before in other studies). Concise descriptions of the chemical schemes are included. The main difference among existing mechanisms is the lumping technique used to classify organic compounds into surrogate groups. First, box model calculations are conducted to highlight the features that lead to differences in the modeled behaviors of photochemical pollutants and their precursors. Results indicate that most chemical schemes yield similar ozone concentrations. Nevertheless, there are significant discrepancies, mainly in predicted concentration of HNO_3, HO_2 and total PAN among model simulations. Finally, the sources of the discrepancy are identified.

Keywords: Air quality models; Atmospheric chemistry; Modeling; Ozone; Kinetic mechanisms

1. Introduction

One of the most important components of air quality models (AQMs) is the photochemical mechanism. A photochemical mechanism for tropospheric chemistry is a mathematical description of photochemical processes of the lower atmosphere through a series of chemical reactions involving primary and secondary pollutants. Photochemical mechanisms used in AQMs are not described in full detail because chemical reactions produce a large number of intermediate non-stable compounds, which disappear quickly and are difficult to detect because of a lack of adequate instrumentation. In addition, the large amount of potential species inhibits the creation of a fully described mechanism from a computational standpoint. Species considered in a photochemical mechanism are categorized as inorganic compounds (NO_x, O_x, HO_x, and SO_x) and organic compounds, mainly volatile organic compounds (VOCs). The variety of VOCs emitted to the atmosphere is wide, and its spatial and temporal speciation in emission inventories is complex. Because of the lack of detailed information about VOCs in emission inventories, species in the chemical mechanism are not usually explicit, but lumped. The implementation of a mechanism into an AQM involves the solution of a highly coupled, non-linear, system of stiff differential equations. The majority of the computing time for tropospheric gas-phase modeling (80–90%) is consumed integrating the chemistry of rate equations (Dennis et al., 1996). Therefore, it is critical to avoid introducing unnecessary complexity into the photochemical mechanism. Divergence points among different chemical schemes are: (1) formulation of the reaction mechanism, (2) rate constants for the reactions and their temperature and pressure dependencies, and (3) temporal integration

*Corresponding author. Tel.: +1-949-824-6126; fax: +1-949-824-8585.
E-mail address: ddabdub@uci.edu (D. Dabdub).

1352-2310/$ - see front matter
doi:10.1016/S1352-2310(03)00567-3

of the reaction rates by the chemical solver (Kuhn et al., 1998). In this paper, the results of a comparison of seven photochemical models are presented. Table 1 lists the mechanism studied, their main characteristics and the AQMs where they are implemented (Russell and Dennis, 2000). Key species followed in this study are O_3, NO, NO_2, NO_3, HNO_3, peroxyacetyl nitrate (PAN), HO_2, H_2O_2 and two organic compounds: ethene and isoprene. The election of these species is based on other works (Gao et al., 1996; Olson et al., 1997; Kuhn et al., 1998; Luecken et al., 1999), and comprises the most important photooxidant species.

2. Previous comparisons of mechanisms

It is well known that different photochemical mechanisms produce dissimilar results. Some authors have compared several schemes throughout the past decade.

Jeffries and Tonnesen (1994) compared the CBM-IV and SAPRC90 using a Lagrangian model, with an analysis method that includes a mass budget to determine the origin of the differences between them. Both mechanisms are based in the same set of experiments of a photochemical smog chambers study. The most important discrepancies were found in high VOC/NO_x ratios, producing a smaller amount of O_3 with CBM-IV.

Poppe et al. (1996) compared 12 chemical mechanisms with numeric simulations in a box model. They used five scenarios, three of them without emissions, to determine the behavior of reactions in the farthest areas from emission sources; and two with emissions. Most mechanisms reported similar O_3 levels. On the other hand, concentrations of PAN, H_2O_2 and NO_3 depended much on the mechanism used. The difference in the prediction of concentrations of ozone among all photochemical mechanisms was of 30%.

Olson et al. (1997) presented the results from the Intergovernmental Panel on Climate Change (IPCC) tropospheric photochemical model intercomparison (PhotoComp). The authors used a 5-day diurnal box model simulation to compare the mixing ratios of O_3, NO, H_2O_2 and diurnal values of HO_2 and OH. Photodissociation rates displayed significant differences, with a root-mean-square (rms) error ranging from ± 6–9% for O_3 and NO_2 to $\pm 15\%$ for H_2O_2 and CH_2O. With in the inclusion of non-methane organic gases in the simulation, O_3 and NO_x means and medians diverged by up to 25%. Models lacking the pressure and water-vapor pathways of the HO_2 self-reactions tended to predict lower H_2O_2 mixing ratios in favor of increased HO_2. Differences in HO_2, in turn, were likely due to the inconsistent reaction rates used by the models for the self-HO_2 reaction to yield H_2O_2, and to differences in the model-calculated photolysis of H_2O_2 and CH_2O.

Kuhn et al. (1998) compared nine chemical mechanisms. The pressure and water-vapor pathways of the HO_2 self-reaction were not included in all mechanisms. Significant differences in H_2O_2 predictions were explained partly by an incorrect use of the HO_2 self-reaction rate constant and by differences in the treatment of the peroxy radical interactions. One of the main conclusions was that most chemical schemes examined yielded similar O_3 concentrations, despite differences in the hydrocarbon lumping. The calculated concentrations of other longer-lived species like H_2O_2 and PAN differed considerably (up to 73%). Also, some of the differences in schemes presented in the comparison reflected differences in numerical solution methods rather than differences in chemistry.

Luecken et al. (1999) examined the production and speciation of reactive oxidized nitrogen (NO_y) from three mechanisms. The most important reaction in NO_y chemistry is the oxidation of isoprene, which influences the production of PAN and organic nitrate. Differences among mechanisms caused large differences in NO_y concentrations. Nitric acid production during the day was consistent among mechanisms. PAN concentration was determined by acyl peroxy radicals (C_2O_3) rates, meanwhile NO_3 prediction for models varied over a large range.

Andersson-Skold and Simpson (1999) described the chemical comparison between the EMEP chemical scheme and a more comprehensive chemical mechanism, the IVL. Despite the divergences in the complexities of the models, predicted ozone levels from both chemical mechanisms were similar for different scenarios. Differences in ozone appeared because of the description of the organic chemistry; IVL treats the chemistry of each VOC in greater depth, including features as $RONO_2$ formation and extensive $RO_2 + RO_2$ chemistry, not included in EMEP. A major difference between the schemes was a higher formation of aldehydes in the IVL scheme, brought about mainly by OH + alkane reactions.

Tonnesen and Luecken (2000) compared SAPRC99 and CB-IV_99 using a Lagrangian model, OZIPR. They found that both mechanisms produce similar predictions for ozone at conditions near the ridgeline of maximum O_3. Nevertheless, CB-IV_99 predicts higher O_3 levels for radical-limited conditions, and SAPRC99 predicts higher ozone concentrations for NO_x-limited conditions. Furthermore, there was considerable temporal variability between the two mechanisms (ozone production is much more rapid in SAPRC99).

Dodge (2000) reviewed five chemical mechanisms used in air quality simulation models (the CBM-IV, the SAPRC mechanism, the RADM2 and RACM models and a new mechanism called the Morphecule

Table 1
Main characteristics of the state-of-the-science photochemical mechanisms

Characteristics	LCC	CBM-IV	RADM2	EMEP	RACM	SAPRC99	CACM
Full Name	Lurmann, Carter and Coyner	Carbon Bond Mechanism, version IV	Regional Acid Deposition Model, version 2	European Monitoring and Evaluation Programme	Regional Atmospheric Chemistry Mechanism	Statewide Air Pollution Research Center, version 99	Caltech Atmospheric Mechanism
Reference	Lurmann et al. (1987)	Gery et al. (1989)	Stockwell et al. (1990)	Simpson et al. (1993)	Stockwell et al. (1997)	Carter (2000b)	Griffin et al. (2002)
Mechanism as implemented in AQM	CIT	Models-3/CMAQ	Models-3/CMAQ	EMEP MSC-W	EURAD	Models-3/CMAQ	CIT
Type	LM[a]	LS[b]	LM[a]	LM[a]	LM[a]	LM[a]	LM[a]
Number of reactions	189	81	156	135	237	198	361
Number of species	72	33	63	64	77	72	191
Constant species	3	2	3	2	4	4	4
Stable inorganic species	12	9	14	11	13	14	15
Inorganic short-lived intermediates	3	5	4	4	4	6	2
Stable organic species	21	6	20	16	24	25	64
Organic short-lived intermediates	14	5	16	26	24	14	65
PAN and analogues	4	1	2	1	2	4	10
Aromatic stable species	9	4	3	2	3	4	24
Biogenic stable species	6	1	1	2	3	1	3

[a] Lumped structure mechanism.
[b] Lumped molecule mechanism.

Mechanism). The mechanisms yielded similar ozone predictions when exercised under clean tropospheric conditions as well as under conditions more representative of polluted boundary layer. Ozone predictions were found to agree within 10%. Nevertheless, concentrations of other oxidants such as H_2O_2 differed considerably.

The novel approaches of this document are that the comparison presented here includes those chemical schemes as used by AQMs with the latest available parameterizations up to date. In addition, CACM mechanism has never been included previously in a comparison work. CACM is a mechanism with an increasing importance since it provides the right speciation of organics necessary for secondary aerosol production.

3. Photochemical mechanisms

A brief description of the mechanisms as implemented in the AQMs depicted in Table 1 is presented in this section, summarizing the main characteristics that should be underlined and that highlighting their differences.

The LCC mechanism is presented in Lurmann et al. (1987). In all, 48 of the species are treated as integrated species in the kinetic solver. Three of the species (M, O_2 and H_2O) are treated as constants and 14 of the species are treated as steady-state species. Aromatic reactions include a parameterized representation of the aromatic ring opening products. PAN analogues from non-α-dicarbonyl products are lumped with PAN analogues formed in other areas of the mechanism. Since the early LCC mechanism did not include biogenic species, the modified scheme used in the CIT Airshed Model (McRae et al., 1992) includes biogenic organic compounds such as isoprene, α-pinene, β-pinene, myrcene, γ-carene and limonene and their reactions with OH, O, NO_3 and ozone, and also revises the oxidation of organic compounds by the reaction with OH, comprising 169 reactions and 65 species.

CBM-IV (Gery et al., 1989) is a lumped-structure condensed mechanism. Carbon bond approach is utilized for the lumping of organic species. The mechanism contains 33 species represented in 81 reactions, and treats the reactions of four different types of species: inorganic species, explicit organic species, organic species represented by carbon surrogates, and organic species that are represented by molecular surrogates. Inorganic chemistry is represented explicitly with no lumping. Organics represented explicitly are formaldehyde, ethene and isoprene. Carbon bond surrogates describe the chemistry of different types of carbon bonds commonly found as parts of larger molecules. CBM-IV is widely used in research and regulatory AQMs as Models-3/CMAQ (Byun and Ching, 1999), and this will be the scheme implemented in this comparison.

RADM2 (Stockwell et al., 1990) is built on the RADM1 scheme (Stockwell, 1986). It includes 156 reactions among 63 species. The most important upgrades include three classes of higher alkanes, a detailed treatment of aromatic chemistry, two higher alkene classes that represent internal and terminal alkenes, treatment of ketones and dicarbonyl species as classes distinct from aldehydes, inclusion of isoprene as an explicit species and a detailed treatment of peroxy radical–peroxy radical reactions. Inorganic species include 14 stable species, four reactive intermediates and three abundant stable species (oxygen, nitrogen and water). H_2 is not included in the mechanism. Atmospheric organic chemistry is represented by 26 stable species and 16 peroxy radicals. VOCs are grouped together into a manageable set of VOC classes based on similarity of oxidation reactivity and emission magnitudes (Middleton et al., 1990). Organic compounds are aggregated into 15 classes of reactive organic species. The implementation of RADM2 in Models-3/CMAQ is analogous to that described by Stockwell et al. (1990) with only two minor modifications: the reaction of OH with cresol was reformulated to eliminate negative stoichiometry in the mechanism, and the concentration of methane is assumed to be constant (Gipson and Young, 1999).

EMEP (Simpson, 1992; Simpson et al., 1993) is of particular importance to policy-related studies in Europe. It uses a lumped molecule approach to represent organic compounds. Each species in the EMEP mechanism represents a range of species of similar structure and reactivity. Photodissociation rates for 13 species are specified in the model as a function of the solar zenith angle. The EMEP version used is based on Simpson et al. (1993), but the isoprene mechanism has been updated, implementing some reactions proposed by Paulson and Seinfeld (1992). EMEP includes reactions of isoprene with OH, NO_3 and ozone. In addition, eight reactions and four species proposed by Simpson (1995) have been added to model the interactions between the peroxy radicals from the isoprene degradation and HO_2. This updated mechanism includes 135 reactions and 64 species, and is used on the EMEP MSC-W AQM (Simpson, 1992, 1995), developed to study formation and transport of ozone over long term periods in Europe.

RACM (Stockwell et al., 1997) is a completely revised version of the RADM2. The mechanism includes 17 stable inorganic species, four inorganic intermediates, 32 stable organic species (four of these are primarily of biogenic origin) and 24 organic intermediates, in 237 reactions. Changes in inorganic chemistry from previous RADM2 mechanism were relatively small. An accurate representation of the production of CO_2 is excluded

both from RADM2 and RACM mechanisms. In RACM, the VOCs are aggregated into 16 anthropogenic and three biogenic model species. The grouping of organic chemical species into the RACM model species is based on the magnitudes of the emission rates, similarities in functional groups and the compound's reactivity toward OH. The organic chemistry was revised significantly. The aromatic chemistry was more widely treated in RACM, including amounts of products from the aromatic-OH addition that had been ignored in RADM2. The oxidation mechanism for isoprene, α-pinene, and d-limonene is more detailed and realistic than that in the RADM2 mechanism. This scheme has been implemented in the EURAD AQM (Hass, 1991).

The latest version of the SAPRC mechanism, designated SAPRC99 (Carter, 2000a) represents a complete update of the SAPRC90 mechanism by Carter (1990). The mechanism has assignments for 400 types of VOCs, and can be used to estimate reactivities for 550 VOC categories. The inorganic reactions in the mechanism are essentially the same as those included in previous versions. A total of 24 model species are used to represent the reactive organic product species: 11 are explicit, and 13 represent groups of similar products using the lumped molecule approach. The PAN analogue formed from glyoxal is lumped with the rest of the higher PAN analogues. Isoprene photooxidation products in the mechanism are included. SAPRC uses a condensed representation of the reactive organic oxidation products and a higher condensed representation of peroxy reactions than does RADM2 or RACM. The SAPRC99 mechanism used in Models-3/CMAQ consists of 72 species in 198 reactions, as described in Carter (2000b).

CACM, developed by Griffin et al. (2002), is the first detailed mechanism directed toward explicit formation of the semivolatile products that could constitute observed secondary organic aerosols (SOAs), and has been implemented in the CIT airshed model. It includes a total of 191 species and 361 reactions: 120 fully integrated species (15 inorganic, 71 reactive organic and 34 unreactive organic), 67 pseudo-steady-state species (two inorganic and 65 organic); and four fixed-concentration species. The inorganic chemistry within CACM is derived primarily from the SAPRC99. Primary organic compounds are lumped in a manner similar to that described by Stockwell et al. (1997). Oxidation reactions of surrogate parents are tracked individually. The lumped model compound corresponding to a given individual parent hydrocarbon is determined by considering the size of the molecule, its structural characteristics, its functionality, its reactivity, and its SOA forming potential. Isoprene is treated explicitly in the CACM, and methyl-vinyl-ketone and methacrolein are major oxidation products of isoprene and are included explicitly. For monoterpenes, CACM incorporates a class (BIOH) for those monoterpenes that have relatively high SOA yield parameters, and another class (BIOL) for those with a relatively low SOA-yield.

4. Methodology

The results presented here correspond to a scenario representing a remote troposphere simulation, since this is the simplest and straightforward case to analyze and one that is consistent with previous studies as described below. This scenario starts from an initial set of trace gas concentrations without emissions, and is sensitive to the details of the formulation of organic species and the rate constants for the reactions in the individual schemes. In addition, this work is focused on elucidating the variability of results among published models, and therefore parameters were chosen to make all mechanisms absolutely comparable. The methods used are similar to those followed by Poppe et al. (2001). The photolysis rate coefficients are calculated for the longitude and latitude of the South Coast Air Basin of California. Simulations account for diurnally dependence of photolysis rate coefficients. The base temperature is 298.16 K, remaining constant during the simulation. Calculations are started at 0 LST and cover the following 24 h; all the same, results show the hours where solar radiation is present, from 6 LST until 18 LST, since photochemical processes are more active at this time of the day. The initial concentrations are derived from Gao et al. (1996) and Seefeld and Stockwell (1999). All depositions are set to zero in order to concentrate on differences in the chemical schemes. Table 2 shows other parameters of the scenarios modeled.

Simulations are performed using a zero-dimensional box model. The stiffness of the system of ordinary differential equations (ODE) requires the use a robust numerical integrator. The VODE library (Brown et al., 1989), in its single precision version (SVODE), is chosen to perform the simulations. Gurciullo et al. (1998), reported that VODE is a factor of two faster than the second most efficient solver included in the comparison for the same tolerated accuracy.

Before summarizing the results, it is worth emphasizing that this works represents a comparison of models. It is impossible to know what 'correct results' should be from any atmospheric chemical scheme. Comparison with smog-chamber data could be a useful complement; nevertheless, smog chambers also represent a very artificial system with many unknown influences. Because of all these reasons, the methodology used in this work proposes the comparison of models with an average tendency, and has been widely supported and applied in the literature (Olson et al., 1997; Kuhn et al., 1998; among others).

Table 2
Parameters specifications and initial conditions (ppm) for scenario

Latitude: 34.058°N	
Longitude: 118.250°W	
Start time: 27 August 1987 (0 h LST)	
Species	Initial concentration (ppm)
NO/NO_x (ppm/ppm)	0.8
NO	0.06664
NO_2	0.01666
O_3	0.03
Ethene	0.0193
Isoprene	0.0007
Formaldehyde	0.02
Lumped aldehydes	0.0147
CO	1.0
Methane	3.0
H_2	0.5
O_2	209,000
N_2	781,000
M	1,000,000
H_2O	15,500
Temperature: 298.16 K	
Pressure: 1013.25 mbar	

5. Results

5.1. Inorganic chemistry of nitrogen oxides and ozone

The kinetics of the gas-phase reactions of inorganic species in the troposphere are relatively well-understood. For instance, O_x–HO_x–NO_x interactions are reflected in a similar way in all mechanisms studied here. Gas-phase inorganic reactions are described, reviewed and evaluated by DeMore et al. (2000) and Atkinson et al. (1999). However, there are a few reactions not fully understood that impact the ability to quantify the formation, cycling and losses of O_3 and NO_x in the troposphere (Atkinson, 2000).

In general, predicted concentrations of NO_x for all models show only small differences (Fig. 1). RADM2 has by far the highest NO concentrations, twice as much as the mean. On the other hand, LCC and CACM mechanisms underpredict NO, yielding 16% less NO than the average. SAPRC99's predictions for NO_2 are 10% higher than the mean and lie on the top of the range. On the other side, LCC shows an averaged prediction of about 9% under the mean values. The explanation of this result is that LCC contains the fastest parameterizations for the transformation of NO_x to nitrate radical and nitric acid; as will be described later, LCC predicts the highest levels of HNO_3. Another significant difference to report is that EMEP mechanism does not include the nitrous acid (HONO) reactions, and this species represents one of the main sources of hydroxyl radical and NO in the troposphere, since HONO is rapidly photolyzed at wavelengths under 400 nm during daytime hours (Finlayson-Pitts and Pitts, 2000).

Ozone concentrations are sensitive to NO and NO_2 concentrations and their reactions in the troposphere (Table 3), and also to the NO_2 photolysis rate and PAN formation and loss rates (Gao et al., 1996). The important reactions responsible for O_3 destruction are directly related to OH and HO_2 chemistry. Fig. 2 shows ozone concentrations during high photochemical activity hours. CACM is the highest-yielding mechanism (values 19% over the average). CACM's predictions are twice as large as those produced by RADM2, which presents a 25% deviation below the average. The maximum deviation of all mechanisms for ozone formation is less than 20% for all simulations. The average deviation is between 1% and 10%. Results obtained show a relation between the dynamics of ozone and hydroperoxide radicals, since those pollutants are coupled through the reaction $O_3 + HO_2 \rightarrow OH + 2O_2$. Most of the model differences with respect to ozone concentrations are traced to differences in the destruction of O_3 due to reaction with HO_2.

5.2. Nitrate radical and nitric acid

The nitrate radical (NO_3) is a strong oxidizing agent and reacts with a number of other atmospheric species. The prerequisite for NO_3 radical production is the simultaneous presence of NO_2 and O_3 in the same air mass. The reaction $NO_2 + O_3 \rightarrow NO_3 + O_2$ is the only primary source of NO_3 in the troposphere (Seinfeld and Pandis, 1998). During daytime, NO_3 rapidly photolyzes and reacts with NO to yield NO_2. In addition, NO_3 reacts with NO_2 during nighttime hours to create N_2O_5. Daytime NO_3 concentrations are shown due to its relation with HNO_3 levels, and since they can provide an idea of the similarity of the photolysis rates included in the mechanisms. The majority of HNO_3 produced in all simulations during daylight hours is through the $OH + NO_2 \rightarrow HNO_3$ reaction, which is one of the most important daytime reactions affecting O_3 and HO_x. During nighttime, N_2O_5 reacts with water vapor to yield HNO_3. As shown in Fig. 3, NO_3 concentrations vary over a large range, and carry high relative deviations with respect to the average. Models result range from the ones predicted by CACM (an average overprediction of 42% in NO_3 values) to the values given by RADM2 (a relative deviation of 52% under the average values). The reason behind such dramatic differences is that the mechanisms implement different NO_3 reactions (Table 3). The gas-phase reaction of NO_3 with water vapor has a minor importance with respect to the heterogeneous reaction of NO_3 with liquid water, and an accurate

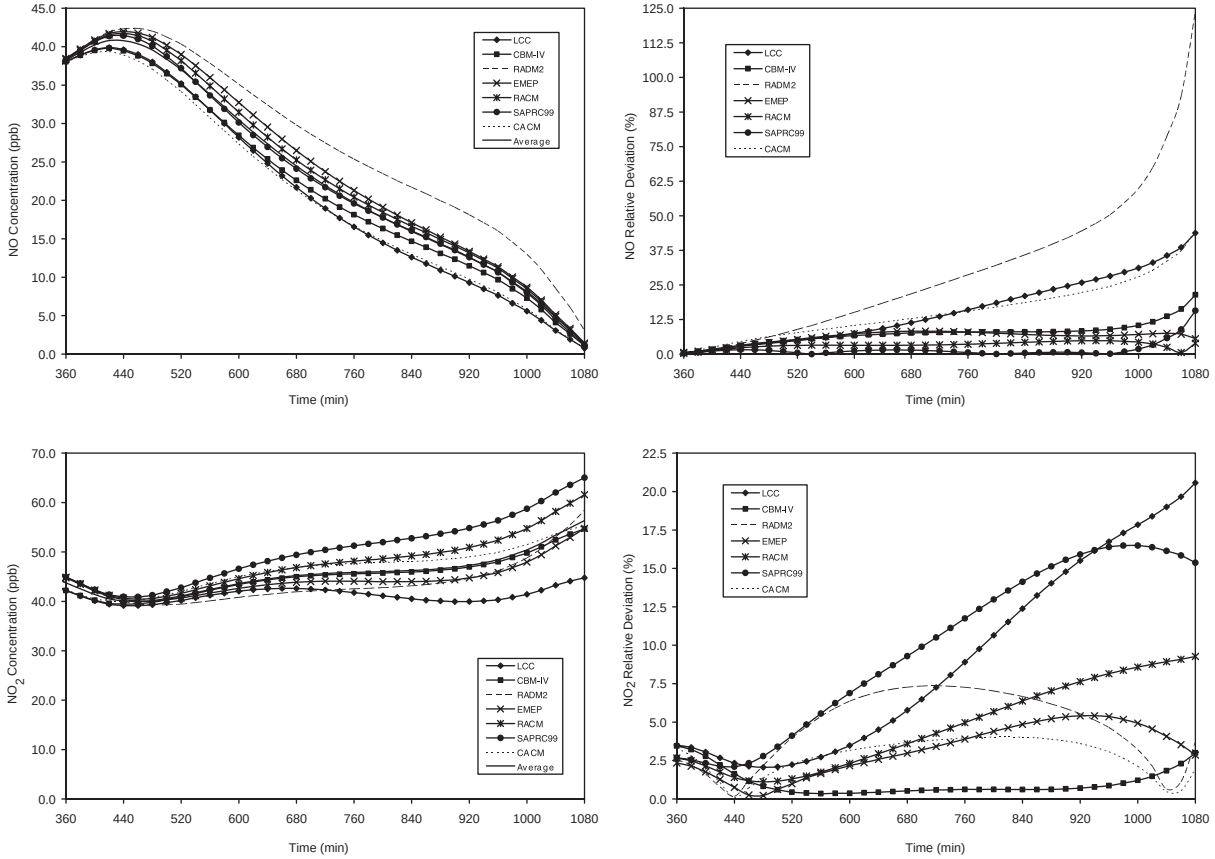

Fig. 1. Simulation results for NO (up) and NO_2 (bottom) concentrations in ppb and relative deviations with respect to the average behavior (%) during daylight hours. Simulation was initiated at 0 h LST with the parameters and initial conditions specified in Table 2.

parameterization for the rate of the heterogeneous reaction is not available. RACM and SAPRC99 include the NO_3 self-reaction, which is not included on the others mechanisms. CBM-IV is the most average-representative model, showing a small deviation with respect to the mean values (a maximum relative deviation of 12% and an average deviation of 7%). Considering nitric acid, there are high uncertainties in the kinetics of the reactions of N_2O_5 with H_2O to form HNO_3. That is why some models (CB-IV, EMEP and RACM) do not include this reaction, presenting a medium-range behavior with respect to HNO_3 (average deviations of 35%, 21% and 40%). The highest deviation from the average is that produced by the LCC, with maximum deviations of 128% and a mean deviation of 61% over the average. On the other extreme, RADM2 underpredicts average values by as much as 50%. Dynamics of HNO_3 are related to those of HO_x, since the reaction of nitrate with hydroperoxyl radical is one of the main sources of HNO_3 in the troposphere, and rate constant differences have important effects on model predictions. The reaction of NO_3 with H_2O_2 to yield HO_2 and nitric acid is included in all mechanisms, but with significant differences in parameterizations that lead to the diverse results presented in the simulations. Differences shown in Fig. 3 for the diverse models are more relevant in the latest hours of the simulation. Nevertheless, production of HNO_3 in the early hours of the simulations is consistent among the mechanisms studied. Production of HNO_3 during the night hours through N_2O_5 reactions is implemented in different ways in the mechanisms. These differences affect not only nitric acid concentrations, but also other products such as PAN, since reactions of NO_3 with carbonyls produce acyl peroxy radicals.

5.3. Peroxyacetyl nitrate

PAN has long been known to be an important atmospheric species. It acts as a reservoir for NO_x and acetyl peroxy radicals (C_2O_3) (Stockwell et al., 1995). PAN and analogues are formed during degradation of aldehydes, by the reaction of alkyl and acyl peroxy radicals with NO_2. The thermal decomposition of PAN leads to the formation of CO_2, NO_2 and peroxy radicals. In turn, the reactions of peroxy radicals lead to

Table 3
Similarities and differences between the chemistry of inorganic species in the chemical schemes

Reaction	LCC	CBM-IV	RADM2	EMEP	RACM	SAPRC99	CACM
NO_x and O_3 chemistry							
$NO_2 + h\nu \rightarrow NO + O$	X	X	X	X	X	X	X
$O_3 + h\nu \rightarrow O + O_2$	X	X	X	X	X	X	X
$O_3 + h\nu \rightarrow OSD + O_2$	X	X	X	X	X	X	X
$HONO + h\nu \rightarrow NO + OH$	X	X	X		X	X	
$HONO + h\nu \rightarrow 0.9NO + 0.1NO_2 + 0.9OH + 0.1HO_2$							X
$HONO + h\nu \rightarrow NO_2 + HO_2$						X	
$HNO_4 + h\nu \rightarrow HO_2 + NO_2$			X				
$O + O_2 + M \rightarrow O_3 + M$	X	X	X	X	X	X	X
$O + NO + M \rightarrow NO_2 + M$		X		X	X	X	X
$O + NO_2 \rightarrow NO + O_2$	X	X	X		X	X	X
$O + O_3 \rightarrow 2O_2$					X	X	X
$OSD + H_2O \rightarrow 2OH$	X		X	X	X	X	X
$OSD + M \rightarrow O + M$	X		X	X	X	X	X
$O_3 + OH \rightarrow HO_2 + O_2$	X	X	X	X	X	X	X
$O_3 + HO_2 \rightarrow OH + 2O_2$	X	X	X	X	X	X	X
$NO + NO + O_2 \rightarrow 2NO_2$	X	X	X		X	X	X
$NO + NO_2 + H_2O \rightarrow 2HONO$		X					
$NO + O_3 \rightarrow NO_2 + O_2$	X	X	X	X	X	X	X
$NO + OH + M \rightarrow HONO + M$	X	X	X		X	X	X
$NO + HO_2 \rightarrow NO_2 + OH$	X	X	X	X	X	X	X
$NO_2 + NO_3 \rightarrow NO + NO_2 + O_2$	X	X	X	X	X	X	X
$NO_2 + HO_2 + M \rightarrow HNO_4 + M$	X	X	X		X	X	X
$HONO + OH \rightarrow NO_2 + H_2O$		X			X	X	X
$HONO + HONO \rightarrow NO + NO_2$		X					
$HNO_4 + M \rightarrow NO_2 + HO_2 + M$	X	X	X		X	X	X
$HNO_4 + OH \rightarrow NO_2 + O_2 + H_2O$	X		X		X	X	X
$SO_2 + OH \rightarrow H_2SO_4 + HO_2$	X		X	X	X	X	X
$CO + OH \rightarrow HO_2 + CO_2$	X	X	X		X	X	X
NO_3 and HNO_3 chemistry							
$NO_3 + h\nu \rightarrow NO + O_2$	X		X	X	X	X	X
$NO_3 + h\nu \rightarrow NO_2 + O$	X		X	X	X	X	X
$NO_3 + h\nu \rightarrow 0.89NO_2 + 0.89\ O + 0.11NO$		X					
$HNO_3 + h\nu \rightarrow NO_2 + OH$			X	X	X	X	
$HNO_4 + h\nu \rightarrow 0.65HO_2 + 0.65NO_2 + 0.35OH + 0.35NO_3$					X		
$HNO_4 + h\nu \rightarrow 0.61HO_2 + 0.61NO_2 + 0.39OH + 0.39NO_3$						X	
$O + NO_2 + M \rightarrow NO_3 + M$	X	X			X	X	X
$NO_2 + O_3 \rightarrow NO_3 + O_2$	X	X	X	X	X	X	X
$NO_2 + OH \rightarrow HNO_3$	X	X	X	X	X	X	X
$NO_2 + H_2O \rightarrow HONO - NO_2 + HNO_3$	X						X
$HNO_3 + OH \rightarrow NO_3 + H_2O$	X	X	X	X	X	X	X
$NO_3 + OH \rightarrow NO_2 + HO_2$					X	X	X
$NO_3 + HO_2 \rightarrow HNO_3 + O_2$	X		X				
$NO_3 + HO_2 \rightarrow 0.8NO_2 + 0.2HNO_3 + 0.8OH + O_2$						X	X
$NO_3 + HO_2 \rightarrow 0.7NO_2 + 0.3HNO_3 + 0.7OH + O_2$					X		
$NO_3 + HO_2 + M \rightarrow HNO_3 + O_2 + M$	X						
$NO_3 + HO_2 + H_2O \rightarrow HNO_3 + O_2 + H_2O$	X						
$NO_3 + H_2O_2 \rightarrow HO_2 + HNO_3$				X			
$NO_3 + NO_3 \rightarrow 2NO_2 + O_2$					X	X	
$NO_3 + NO \rightarrow 2NO_2$	X	X	X	X	X	X	X
$NO_3 + NO_2 + M \rightarrow N_2O_5 + M$	X	X	X	X	X	X	X
$N_2O_5 \rightarrow NO_2 + NO_3$	X	X	X	X	X	X	X
$N_2O_5 + H_2O \rightarrow 2HNO_3$	X		X			X	X
HO_2 and H_2O_2 chemistry							
$H_2O_2 + h\nu \rightarrow 2OH$	X	X	X	X	X	X	X
$HO_2 + OH \rightarrow H_2O + O_2$			X	X	X	X	X
$HO_2 + HO_2 \rightarrow H_2O_2$	X	X	X	X	X	X	X
$HO_2 + HO_2 + H_2O \rightarrow H_2O_2 + O_2 + H_2O$	X	X	X	X	X	X	X
$H_2O_2 + OH \rightarrow HO_2 + H_2O$	X	X	X	X	X	X	X
$OH + H_2 \rightarrow HO_2$				X	X	X	

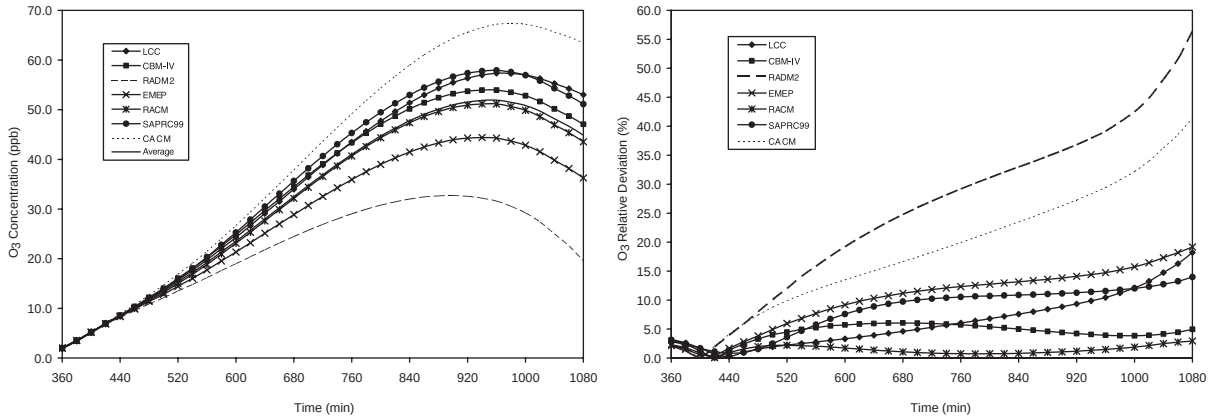

Fig. 2. Simulation results for ozone concentrations (ppb) and relative deviations with respect to the average behavior (%) during daylight hours. Simulation was initiated at 0 h LST with the parameters and initial conditions specified in Table 2.

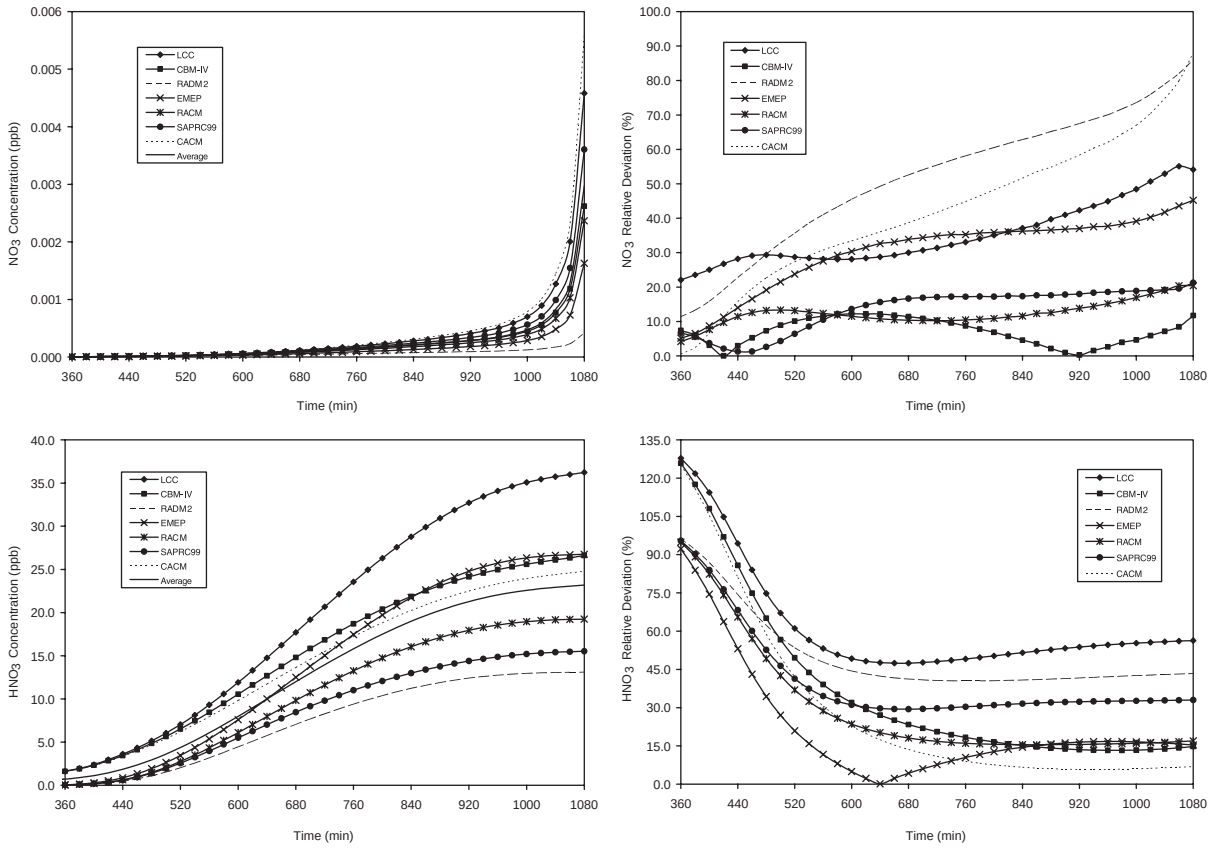

Fig. 3. Simulation results for NO_3 (up) and HNO_3 concentrations (bottom) in ppb and relative deviations with respect to the average behavior (%) during daylight hours. Simulation was initiated at 0 h LST with the parameters and initial conditions specified in Table 2.

production of HO_2 and formaldehyde, which contribute to photochemical reactions including ozone formation. Therefore, variations of PAN are related to those of ozone with respect to time of the day, but not with respect to amplitude (Grosjean et al., 2001). Results obtained from this study show that peak concentrations of PAN precede those of ozone by 1 h, as depicted in Figs. 2 and 4. Peroxy nitrate species are treated differently in the mechanisms under study (Table 4). For instance, CACM considers 10 different peroxy

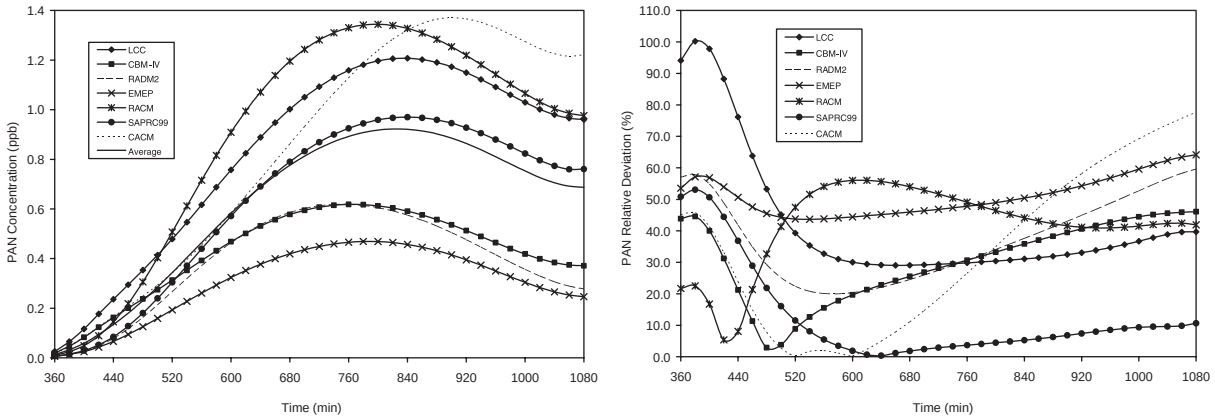

Fig. 4. Simulation results for total PAN concentrations (ppb) and relative deviations with respect to the average behavior (%) during daylight hours. Simulation was initiated at 0 h LST with the parameters and initial conditions specified in Table 2.

Table 4
Peroxy nitrate species included in the mechanisms

Reaction	LCC	CBM-IV	RADM2	EMEP	RACM	SAPRC99	CACM
Peroxy pentionyl nitrate							X
Peroxyacetyl nitrate (PAN)	X	X	X	X	X	X	X
Unsaturated PANs			X		X		
Peroxy propionyl nitrate (PPN)	X					X	X
Keto-PPN							X
Methylene-PPN (derived from methacrolein)				X		X	X
Peroxy nitrate derived from glyoxal							X
Peroxy 3-methyl-heptionyl nitrate							X
Peroxy 2-hydroxy-3-isopropyl-6-keto-heptionyl nitrate							X
Peroxy 3-isopropyl-4-hydroxy-2-butenionyl-nitrate (PAN analogue derived from aromatic aldehydes)						X	X
Peroxy nitrate derived from glyoxalic acid							X

nitrates depending on the source of the species. EMEP distinguishes between PAN and a peroxy methacroleinyl nitrate. Meanwhile, LCC and CBM-IV consider just the PAN. SAPRC99 considers also peroxy propionyl nitrate and other higher alkyl PAN analogues, PAN analogues formed from aromatic aldehydes and a PAN analogue formed from methacrolein. RADM2 and RACM lump peroxy nitrates into PAN and higher saturated PANs, and unsaturated PANs. Simulations results, shown in Fig. 4, illustrate that the amount of total PAN species formed by the various chemical schemes differs considerably. RADM2 presents the lowest PAN values, with a maximum deviation with respect to mean mechanisms' value around 60%. On the other side, RACM and CACM yield the highest PAN levels, with a maximum deviation of 53% and 78%, respectively. The most representative mechanism with respect to average predictions is SAPRC99, with a mean relative deviation of 12%. Peroxy nitrate formation and decay rates differ substantially among the mechanisms, and depend on the magnitude of the competing reactions of C_2O_3 radical, which differs in their implementation in the different mechanisms. The yield of PAN is affected strongly by the choice of rate parameters (Kley et al., 1999). While the rate of PAN formation is similar among the mechanism considered, there are various differences in the implementation of PAN decomposition. For example, in most mechanisms (CBM-IV, RADM2, RACM, SAPRC99, CACM), PAN yields the corresponding acyl peroxy radical and NO_2 through an equilibrium reaction, but chemical kinetics differ considerably. EMEP treats the formation of PAN as a fixed-rate reaction. On the other hand, LCC and EMEP include PAN decomposition as a strong temperature-dependent reaction, considering similar kinetics parameters. Luecken et al. (1999) reported that reactions of NO_3 with carbonyls, mainly acetaldehyde, lead to peroxy radicals, which react with NO_2 to yield peroxynitrates. Therefore, not only NO_3 but also aldehyde considerations in the mechanisms influence PAN concentrations. CACM and LCC use similar kinetics for the reaction of aldehydes with NO_3, and this reaction rate is the highest for all the mechanisms compared, which explains the highest levels of PAN production shown in Fig. 4

(average overpredictions of 42% and 33%, respectively). In contrast, CBM-IV and EMEP use the slowest rates. As a result, PAN concentrations are also the lowest, underestimating the average values by 30% and 51%. RADM2, RACM and SAPRC99 present similar kinetic considerations, but show different behaviors due to differences in aldehydes concentrations reported by the models. RADM2 yields the lowest aldehyde concentrations, which reflects in a lower PAN concentrations with respect to the other two models with similar reaction rates.

5.4. Hydrogen peroxide and hydroperoxyde radical

Hydrogen peroxide (H_2O_2) and hydroperoxide radical (HO_2) are photochemical products that serve as precursors of odd-oxygen as well as reservoirs of odd-hydrogen radicals. The generation of H_2O_2 and HO_2 is affected by the levels of chemical components such as NO_x, CO, methane and non-methane hydrocarbons (Lee et al., 2000). H_2O_2 and organic peroxides chemistry is a weak point in most mechanisms, because of the many complex reactions and possible unknowns that are important under low NO_x/VOC ratio conditions (Kuhn et al., 1998). All mechanisms implement similar reactions for hydrogen peroxide: the bimolecular combination of HO_2, H_2O_2 photolysis and the reaction of H_2O_2 with OH to regenerate HO_2 radicals (Table 3). Furthermore, kinetic constants and reaction rates are similar for all mechanisms. HO_2 self-reaction is the only important gas-phase source of hydrogen peroxide in the troposphere. As a result, HO_2 and H_2O_2 concentrations are closely related. Rates for this reaction are identical in CACM and SAPRC99; RADM2, EMEP and RACM use the expression referenced in DeMore et al. (2000); LCC and CBM-IV differ from the rest in kinetics considerations. Fig. 5 shows that differences among the mechanisms are important. RADM2 predicts the lowest concentrations of HO_2 and H_2O_2, with production rates that are 53% and 71% lower than the mean, and showing maximum relative deviations of 95% and 85%, respectively. These deviations are due to the explicit treatment of HO_2 and organic peroxide radicals in the model (Stockwell, 1995). On the other hand, LCC

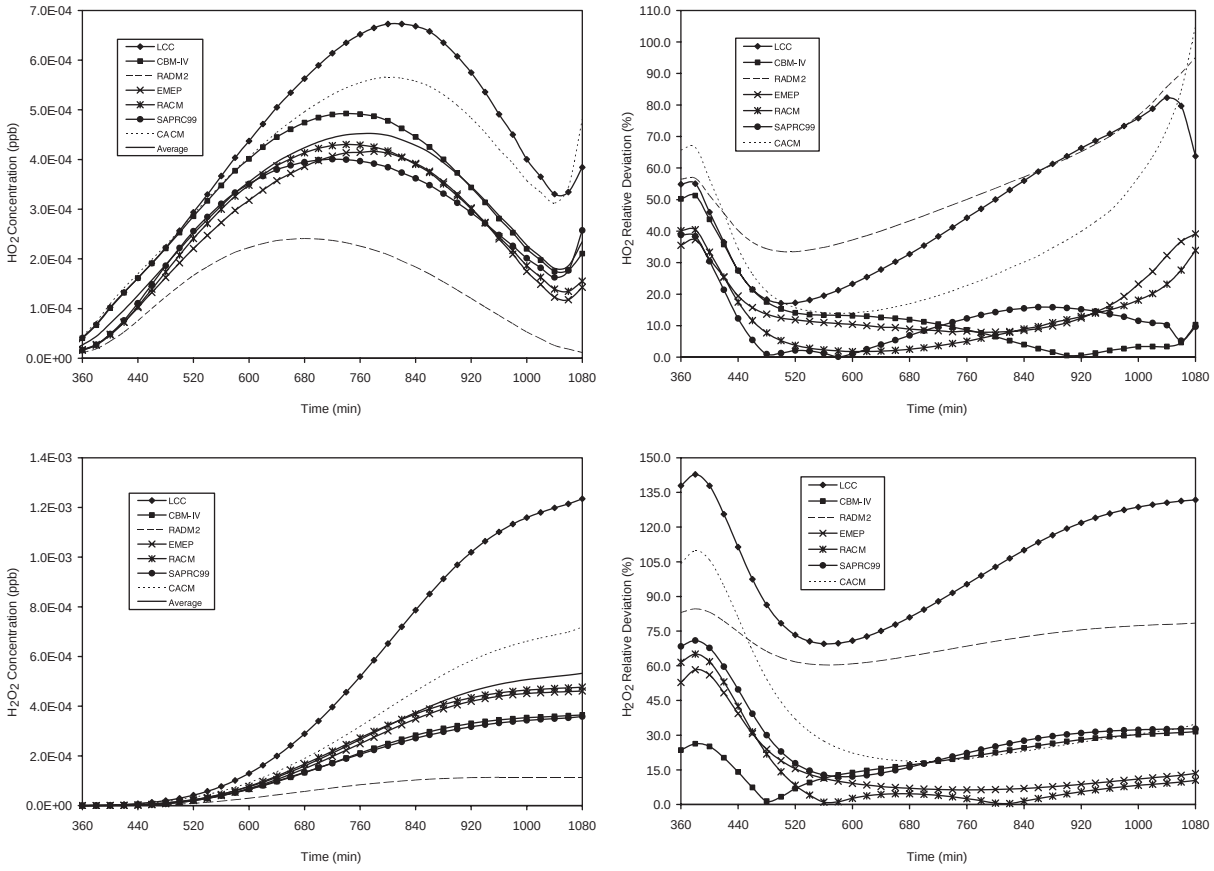

Fig. 5. Simulation results for HO_2 (up) and H_2O_2 (bottom) concentrations in ppb and relative deviations with respect to the average behavior (%) during daylight hours. Simulation was initiated at 0 h LST with the parameters and initial conditions specified in Table 2.

parameterizations lead to the highest peroxide values, producing average deviations of 46% for HO_2 and 92% for H_2O_2. The mechanism that predicts concentrations closest to the average is SAPRC99 for HO_2 (underestimation of 11%) and RACM for H_2O_2 (underestimation of 13%). Differences among all mechanisms originate from different considerations of water-vapor dynamics. HO_2 and OH concentrations are overpredicted by the HO_2 and HO_2 reaction when water vapor is not considered, which leads to an underestimate of gas-phase hydrogen peroxide formation rates and to an overestimate of ozone and organic peroxide formation rates (Stockwell, 1995).

5.5. Alkenes

In the troposphere, alkenes react with atomic oxygen, OH radicals, NO_3 radicals and ozone through the double bonded carbons (Atkinson, 2000). The reasons for focusing on ethene and isoprene in this study are diverse. Both are significant contributors to PAN and organic nitrate formation (Luecken et al., 1999). Ethene is the simplest alkene emitted from anthropogenic sources, and because of its high reactivity with respect to ozone formation, it is included explicitly in all mechanisms. Isoprene is the most significant biogenic compound, and its chemistry is analogous to that of alkenes. Chemicals schemes in this work aggregate biogenic stable species attending to different criteria (Table 5). CACM classifies biogenics attending to the potential to generate SOAs, meanwhile most mechanisms include only isoprene, and LCC and RACM treat species explicitly as pinene, limonene, myrcene and carene. Isoprene is considered in all mechanisms because of its importance in photochemical chemistry. As shown in Fig. 6, ethene parameterization is similar in all mechanisms. The oldest mechanisms (LCC, RADM2 and CBM-IV) produce higher relative deviations, which

Table 5
Reactions of biogenic stable species included in the mechanisms

Reaction	Biogenic stable species chemistry						
	LCC	CBM-IV	RADM2	EMEP	RACM	SAPRC99	CACM
Isoprene + OH	X	X	X	X	X	X	X
Isoprene + NO_3	X	X	X	X	X	X	X
Isoprene + O_3	X	X	X	X	X	X	X
Isoprene + O	X	X			X	X	X
APIN[a] + OH	X				X		
APIN + NO_3	X				X		
APIN + O_3	X				X		
BPIN[b] + OH	X						
BPIN + NO_3	X						
BPIN + O_3	X						
LIM[c] + OH	X				X		
LIM + NO_3	X				X		
LIM + O_3	X				X		
Myrcene + OH	X						
Myrcene + NO_3	X						
Myrcene + O_3	X						
γ-Carene + OH	X						
γ-Carene + NO_3	X						
γ-Carene + O_3	X						
BIOL[d] + OH							X
BIOL + NO_3							X
BIOL + O_3							X
BIOL + O							X
BIOH[e] + OH							X
BIOH + NO_3							X
BIOH + O_3							X
BIOH + O							X

[a] α-Pinene and other cyclic terpenes with one double bond.
[b] β-Pinene.
[c] d-Limonene and other cyclic diene-terpenes.
[d] Low SOA monoterpene species (α-terpineol).
[e] High SOA monoterpene species (γ-terpinene).

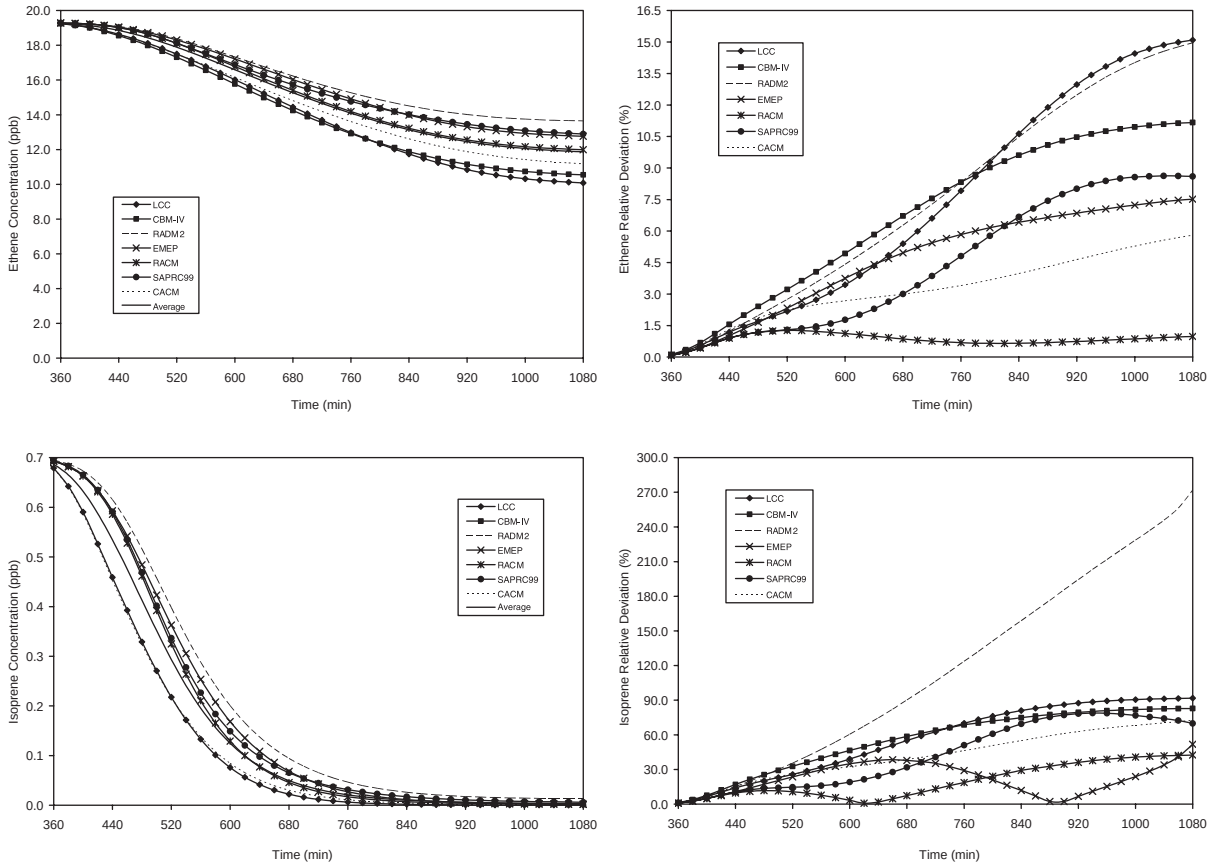

Fig. 6. Simulation results for ethene (up) and isoprene (bottom) concentrations in ppb and relative deviations with respect to the average behavior (%) during daylight hours. Simulation was initiated at 0 h LST with the parameters and initial conditions specified in Table 2.

are no larger than 16%. The kinetics of ethene are slower for RADM2, meanwhile LCC is the most-rapidly reactive mechanism. EMEP and SAPRC99 implement similar parameterizations. Minimum deviations are under 2% for RACM, which would be the average-representative model. Isoprene is highly reactive in the atmosphere, and its lifetime is relatively short when compared to other organic species as ethene. Mechanisms that do not include atomic oxygen reaction with isoprene (RADM2 and EMEP) yield the highest over-predictions (115% and 22% with respect to the average). LCC and CACM levels are under the average values (57% and 43%). Finally, RACM yields the smallest deviations with respect to the mean, around 20%. One of the sources of the alkenes discrepancy among mechanisms is the alkene reaction with O^3P, since RADM2 and EMEP do not include it in their schemes. Its importance derives from the fact that the kinetic constant of the alkene + O^3P is of the same order of magnitude as the alkene + OH and greater than the alkene + O_3 kinetic constant.

6. Summary and conclusions

A comparison of photochemical mechanisms for air quality modeling is presented. Predictions of different tropospheric reaction mechanisms for a common set of initial and boundary conditions are compared to identify factors affecting the accuracy of reactivity simulations. The range of concentrations predicted by the box mechanisms show the state-of-the-science in tropospheric chemistry. All the chemical schemes are used as part of chemical transport models, and the main conclusions of the results are summarized as follows: (1) NO_x does not show important differences, except in the case of RADM2, since all the mechanisms relied on the same kinetic and mechanistic data for inorganic chemistry. EMEP mechanism does not include the HONO chemistry. RADM2 implements the oldest parameterizations considered in this comparison (LCC and CBM-IV are older mechanisms, but their chemistry has been revised). As a result, NO concentrations predicted by RADM2 deviate with respect to the

average. (2) The mechanisms that tend to predict higher ozone concentrations are CACM and LCC. This high O_3-productivity is accompanied by a high formation of organic hydroperoxides. Deviations in predicted ozone concentrations among the models are due to different consideration in mechanisms' compounds. This effect becomes more pronounced for reactive species producing a high yield of aldehydes, and thereby PAN and analogues. (3) NO_3 concentrations vary over a large range for the different mechanisms, and present high relative deviations with respect to the average. An explanation may come from the different NO_3 reactions considered in the models. HNO_3 tendency is also strongly related to that of HO_x, since the reaction of nitrate with hydroperoxyl radical is the main source of HNO_3 in the troposphere. $NO_3 + HO_2$ is included in all mechanisms, but with important differences in parameterizations that lead to the diverse results found in the simulations. (4) Divergence between different mechanisms in the case of total PAN is important, since the yield of total PAN is affected by the choice of rate parameters. Peroxy nitrate formation and decay rates differ substantially among the diverse mechanisms, as well as C_2O_3 radical reactions. (5) The differences in hydroperoxide and hydrogen peroxide are relevant, and are traced to the inconsistent conversion rates for HO_2 to H_2O_2 reaction and to the water-vapor concentration dependences of the HO_2 self-reaction. (6) Alkenes chemistry is consistent among the models considered in this comparison, and does not show important differences. Most mechanisms include similar kinetics parameterizations for ethene and isoprene, and the only important divergence comes from the fact that the reaction of these compounds with atomic oxygen is not considered in all models.

Results obtained in this work are summarized in Table 6. They are consistent with other comparison exercises found in the bibliography and previously exposed in Section 2. The conclusions from this model comparison confirms that even for the simulation of

Table 6
Comparison of the deviation of mechanisms' results with respect to the average value

Species		% deviation of individual mechanisms from average values						
		LCC	CBM-IV	RADM2	EMEP	RACM	SAPRC99	CACM
NO	Max	−43.8	−21.4	+123.8[a]	+8.3	+4.9[b]	+15.7	−44.6
	Average	−15.7	−7.4	+30.0[a]	+6.3	+3.3	−1.5[b]	−15.6
NO_2	Max	−20.6[a]	−3.5[b]	−7.4	−5.4	+9.3	+16.5	+4.1
	Average	−8.9	−1.0[b]	−4.7	−3.2	+4.7	+10.0[a]	+2.8
O_3	Max	+18.2	+6.0	−56.4[a]	−19.2	−2.9[b]	+14.0	+41.4
	Average	+6.2	+4.4	−25.4[a]	−10.4	−1.4[b]	+8.3	+18.6
NO_3	Max	+55.6	−12.3[b]	−86.0	−45.2	−20.9	+21.3	+88.0[a]
	Average	+35.0	−7.1[b]	−51.8[a]	−30.5	−12.5	+13.4	+42.1
HNO_3	Max	+127.8[a]	+125.9	−96.2	−92.3[b]	−94.9	−95.4	+125.2
	Average	+61.4[a]	+35.5	−49.8	+21.4[b]	−29.1	−40.0	+27.9
PAN	Max	+100.7[a]	+46.1[b]	−59.6	−64.2	+56.1	−53.1	+77.7
	Average	+41.8	−30.1	−37.1	−50.8[a]	+42.0	+12.2[b]	+33.0
HO_2	Max	+83.2	+51.5	−95.1	−39.3	−41.0	−39.3[b]	+105.0[a]
	Average	+45.7	+12.5	−53.2[a]	−15.7	−11.8	−11.1[b]	+34.5
H_2O_2	Max	+142.8[a]	−31.5[b]	−84.7	−58.7	−65.1	−71.0	+110.0
	Average	+103.4[a]	−20.3	−70.8	−15.6	−12.6[b]	−29.1	+36.9
Ethene	Max	−15.1[a]	−11.2	+15.0	+7.5	+1.3[b]	+8.6	−5.8
	Average	−7.3	−6.8	+7.5[a]	−4.7	+0.9[b]	+4.4	−3.3
Isoprene	Max	−91.8	+82.8	+271.8[a]	+51.8	+42.5[b]	+79.0	−72.7
	Average	−56.7	+55.8	+115.3[a]	+22.3	+19.7[b]	+43.2	−42.5

[a] Maximum deviations with respect to the average value.
[b] Minimum deviations with respect to the average value.

extremely simple situations, there can be discrepancies in predicted concentrations. Furthermore, this study shows that such discrepancies are significant in most of the cases and quantifies typical biases among various mechanisms.

References

Andersson-Skold, Y., Simpson, D., 1999. Comparison of the chemical schemes of the EMEP MSC-W and IVL photochemical trajectory models. Atmospheric Environment 33 (7), 1111–1129.

Atkinson, R., 2000. Atmospheric chemistry of VOCs and NO_x. Atmospheric Environment 34, 2063–2101.

Atkinson, R., Baulch, D.L., Cox, R.A., Hampson Jr., R.F., Kerr, J.A., Rossi, M.J., Troe, J., 1999. Evaluated kinetic and photochemical data for atmospheric chemistry, organic species: supplement VII. Journal of Physical and Chemical Reference Data 28, 191–393.

Brown, P.N., Byrne, G.D., Hindmarsh, A.C., 1989. VODE: a variable-coefficient ODE solver. Journal on Scientific and Statistical Computing 10 (5), 1038–1051.

Byun, D.W., Ching, J.K.S. (Eds.), 1999. Science algorithms of the EPA Models-3 Community Multiscale Air Quality (CMAQ) modeling system. EPA Report No. EPA-600/R-99/030, Office of Research and Development. US Environmental Protection Agency, Washington, DC.

Carter, W.P.L., 1990. A detailed mechanism for the gas-phase atmospheric reactions of organic compounds. Atmospheric Environment 24A, 481–518.

Carter, W.P.L., 2000a. Documentation on the SAPRC-99 chemical mechanism for VOC reactivity assessment. Final Report to California Air Resources Board Contract No. 92-329 and 95-308, May 2000.

Carter, W.P.L., 2000b. Implementation of the SAPRC-99 chemical mechanism into the Models-3 Framework. Report to the US Environmental Agency, 29 January 2000.

DeMore, W.B., Sander, S.P., Friedl, R.P., Golden, D.M., Hampson, R.F., Kurylo, M.J., Howard, C.J., Ravishankara, A.R., Kolb, C.E., Moortgart, G.K., Molina, M.J., 2000. Chemical kinetics and photochemical data for use in stratospheric modeling. Supplement to Evaluation 12: update of key reactions. In: Evaluation 13, NASA Panel for Data Evaluation. Jet Propulsion Laboratory Publication 00-3, Pasadena, CA, 9 March.

Dennis, R.L., Byun, D.W., Novak, J.H., Gallupi, K.J., Coats, C.J., Vouk, M.A., 1996. The next generation of integrated air quality modeling: EPA's Models-3. Atmospheric Environment 30 (12), 1925–1938.

Dodge, M.C., 2000. Chemical oxidant mechanisms for air quality modeling: critical review. Atmospheric Environment 34 (12–14), 2103–2130.

Finlayson-Pitts, B.J., Pitts, J.N., 2000. Chemistry of the Upper and Lower Atmosphere. Theory, Experiments and Applications. Academic Press, New York, UK, p. 969.

Gao, D., Stockwell, W.R., Milford, J.B., 1996. Global uncertainty analysis of a regional-scale gas-phase chemical mechanism. Journal of Geophysical Research 101, 9107–9119.

Gery, M.W., Whitten, G.Z., Killus, J.P., Dodge, M.C., 1989. A photochemical kinetics mechanism for urban and regional scale computer modeling. Journal of Geophysical Research 94 (D10), 12925–12956.

Gipson, G.L., Young, J.O., 1999. Gas-phase chemistry. In: Byun, D.W., Ching, J.K.S. (Eds.), Science Algorithms of the EPA Models-3 Community Multiscale Air Quality System (CMAQ) Modeling System. US Environmental Protection Agency, Atmospheric Modeling Division, Research Triangle Park, NC, EPA 600/R-99/030.

Griffin, R.J., Dabdub, D., Seinfeld, J.H., 2002. Secondary organic aerosol, 1. Atmospheric chemical mechanism for production of molecular constituents. Journal of Geophysical Research 107, 4332–4357.

Grosjean, E., Grosjean, D., Woodhouse, L.F., 2001. Peroxyacetyl nitrate and peroxypropionyl nitrate during SCOS 97-NARSTO. Environmental Science and Technology 35, 4007–4014.

Gurciullo, C.S., Pandis, S.N., Kumar, N., Lurmann, F.W., 1998. Development and testing of an aqueous-phase chemistry module for Eulerian chemical transport models. Final Report prepared for the Coordinating Research Council, Atlanta, GA by Carnegie Mellon University, Pittsburgh, PA and Sonoma Technology, Inc., Petaluma, CA, STI-997510-1822-FR, June 1998.

Hass, H., 1991. Description of the EURAD chemistry transport module (CTM) version 2. In: Ebel, A., Neubauer, F.M., Speth, P. (Eds.), Report 83. Institute of Geophysics and Meteorology, University of Cologne, Cologne, Germany.

Jeffries, H.F., Tonnesen, J., 1994. A comparison of two photochemical reaction mechanisms using mass balance and process analysis. Atmospheric Environment 28, 2991–3003.

Kley, D., Kleinmann, M., Sanderman, H., Krupa, S., 1999. Photochemical oxidants: state of the science. Environmental Pollution 100, 19–42.

Kuhn, M., Builtjes, P.J.H., Poppe, D., Simpson, D., Stockwell, W.R., Andersson-Skold, Y., Baart, A., Das, M., Fiedler, F., Hov, O., Kirchner, F., Makar, P.A., Milford, J.B., Roemer, M.G.M., Ruhnke, R., Strand, A., Vogel, B., Vogel, H., 1998. Intercomparison of the gas-phase chemistry in several chemistry and transport models. Atmospheric Environment 32, 693–709.

Lee, M., Heikes, B.G., O'Sullivan, D.W., 2000. Hydrogen peroxide and organic hydroperoxide in the troposphere: a review. Atmospheric Environment 34, 3475–3494.

Luecken, D.J., Tonnesen, G.S., Sickles, J.E., 1999. Differences in NO_y speciation predicted by three photochemical mechanisms. Atmospheric Environment 33 (7), 1073–1084.

Lurmann, F.W., Carter, W.P.L., Coyner, L.A., 1987. A surrogate species chemical reaction mechanism for urban-scale air quality simulation models. Report prepared for the US Environmental Protection Agency Contract No. 68-02-4104, Research Triangle Park, NC, EPA 600/3-87/014.

McRae, G.J., Russell, A.G., Harley, R.A., 1992. CIT Photochemical Airshed Model—Systems Manual. Carnegie Mellon University, Pittsburgh, PA, and California Institute of Technology, Pasadena, CA, February 1992.

Middleton, P., Stockwell, W.R., Carter, W.P.L., 1990. Aggregation of volatile organic compound emissions for regional modeling. Atmospheric Environment 6, 1107–1133.

Olson, J., Prather, M., Berntsen, T., Carmichael, G., Chatfield, R., Connell, P., Derwent, R., Horowitz, L., Jin, S., Kanakidou, M., Kasibhatla, P., Kotamarthi, R., Kuhn, M., Law, K., Penner, J., Perliski, L., Sillman, S., Stordal, F., Thompson, A., Wild, O., 1997. Results from the intergovernmental panel on climate change (IPCC) photochemical model intercomparison (PhotoComp). Journal of Geophysical Research 102, 5979–5991.

Paulson, S.E., Seinfeld, J.H., 1992. Development and evaluation of a photooxidation mechanism for isoprene. Journal of Geophysical Research 97, 20703–20715.

Poppe, D., Andersson-Skold, Y., Baart, A., Builtjes, P.J.H., Das, M., Hov, O., Kirchner, F., Kuhn, M., Makar, P.A., Milford, J.B., Roemer, M.G.M., Ruhnke, R., Simpson, D., Stockwell, W.R., Strand, A., Vogel, B., Vogel, H., 1996. Intercomparison of the gas-phase chemistry of several numerical chemistry and transport models. In: EUROTRAC Special Report 1996, Garmisch-Partenkirchen, Germany.

Poppe, D., Aumont, B., Ervens, B., Geiger, H., Herrmann, H., Roth, E.-P., Seidl, W., Stockwell, W.R., Vogel, B., Wagner, S., Weise, D., 2001. Scenarios for modeling multiphase tropospheric chemistry. Journal of Atmospheric Chemistry 40, 77–86.

Russell, A., Dennis, R., 2000. NARSTO critical review of photochemical models and modeling. Atmospheric Environment 34, 2283–2324.

Seefeld, S., Stockwell, W.R., 1999. First-order sensitivity analysis of models with time-dependent parameters: an application to PAN and ozone. Atmospheric Environment 33, 2491–2953.

Seinfeld, J.H., Pandis, S.N., 1998. Atmospheric Chemistry and Physics: from Air Pollution to Climate Change. Wiley, New York, p. 1326.

Simpson, D., 1992. Long period modeling of photochemical oxidants in Europe, calculation for July 1985. Atmospheric Environment 26A (9), 1609–1634.

Simpson, D., 1995. Biogenic emissions in Europe, 2. Implication for ozone control strategies. Journal of Geophysical Research 100 (D11), 22891–22906.

Simpson, D., Andersson-Skold, Y., Jenkin, M.E., 1993. Updating the chemical scheme for the EMEP MSC-W oxidant model: current status. EMEP MSC-W note 2/93. Norwegian Meteorological Institute, Oslo, Norway.

Stockwell, W.R., 1986. A homogeneous gas phase mechanism for use in a regional acid deposition model. Atmospheric Environment 20, 1615–1632.

Stockwell, W.R., 1995. On the HO_2+HO_2 reaction: its misapplication in atmospheric chemistry models. Journal of Geophysical Research 100 (D6), 11695–11698.

Stockwell, W.R., Middleton, P., Chang, J.S., Tang, X., 1990. The second generation regional acid deposition model chemical mechanism for regional air quality modeling. Journal of Geophysical Research 95, 16343–16367.

Stockwell, W.R., Milford, J.B., Gao, D., Yang, Y.J., 1995. The effect of acetyl peroxy–peroxy radical reactions on peroxyacetyl nitrate and ozone concentrations. Atmospheric Environment 29 (14), 1591–1599.

Stockwell, W.R., Kirchner, F., Kuhn, M., Seefeld, S., 1997. A new mechanism for regional atmospheric chemistry modeling. Journal of Geophysical Research 102 (D22), 25847–25879.

Tonnesen, G.S., Luecken, D., 2000. Intercomparison of photochemical mechanisms using response surfaces and process analysis. In: Millennium NATO/CCMS International Meeting on Air Pollution Modeling and its Application, 15–19 May 2000. American Meteorological Society, Boulder, CO, USA.